Computer Physics Communications 185 (2014) 1564–1569

Contents lists available at ScienceDirect

Computer Physics Communications

journal homepage: www.elsevier.com/locate/cpc

An effective capacitance model for computing the electronic properties of charged defects in crystals

Tzu-Liang Chan [a,b], Alex J. Lee [b,c], James R. Chelikowsky [b,c,d,*]

[a] Department of Physics, Hong Kong Baptist University, Kowloon Tong, Kowloon, Hong Kong

[b] Center for Computational Materials, Institute for Computational Engineering and Sciences, University of Texas, Austin, TX 78712, USA

[c] Department of Chemical Engineering, University of Texas, Austin, TX 78712, USA

[d] Department of Physics, University of Texas, Austin, TX 78712, USA

ARTICLE INFO

Article history:
Received 21 November 2013
Received in revised form
13 February 2014
Accepted 18 February 2014
Available online 26 February 2014

Keywords:
Defect
Ionization
Capacitance
Work function
Density-functional calculation

ABSTRACT

By examining how a defect within a crystalline material responds to small changes in its charge state, the electronic properties of an ionized defect can be modeled by an effective work function and capacitance. Such an approach leads to a correction formula to the total energy of a charged periodic system and allows a comparison between the electronic band structure of the ionized defect to its corresponding neutral one. The correction formula can be related to the potential alignment method and Makov–Payne correction widely adopted in charged periodic systems. The new approach suggests both an alternative interpretation and improvements to the popular Makov–Payne and potential alignment scheme. P-doped Si, which has a shallow donor level, and an isolated vacancy in crystalline Si, which has a deep defect level within the Si energy gap, are chosen as prototypical systems to demonstrate our method.

1. Introduction

The ability to examine theoretically the ionization of defects and dopants in semiconductors is critical to the understanding and development of many applications. Semiconductors are intentionally doped with impurities which can be thermally ionized to generate charge carriers. Unintentional structural defects and impurities can trap charge carriers, and the ionizations waste energy as heat for both electronics and photovoltaic materials. A detailed understanding of defect ionization can aid in the design and optimization of such devices. Electronic structure simulations of defects in crystalline materials are accomplished by a supercell approach where the defect is periodically repeated to minimize surface effects. Unfortunately, this poses serious problems to the study of charged defects since the Coulomb interaction is long-ranged leading to a divergence in the total energy of a charged periodic system [1]. The divergence is relieved by introducing a neutralizing jellium background into the supercell [2]. However, there is an artificial dependence of the ionization energy on the supercell size L owing to the jellium background. One popular attempt to remove such an artifact is the Makov–Payne (MP) correction [3–5], which considers the electrostatic multipole interaction between charged periodic unit cells and arrives at a convenient correction formula for the total energy. The total energy can also be corrected by finite-size scaling, where the L dependence is extrapolated to infer the asymptotic value [4,5]. The interaction between the multipoles can be removed by introducing atom-centered Gaussian charges [6] or local moments to counter the multipole moments [7,8] within the unit cell. For aperiodic (such as molecules) or partially periodic systems (such as nanowires and nanofilms), interaction between unit cells can be reduced by restricting the wave functions [9–11] or truncating the electrostatic potential [12–14] along the aperiodic directions. There are specific schemes that address partially periodic systems [15], such as charged nanowires [16,17] and surfaces [18–21].

In the supercell approach adopted in typical plane-wave codes for electronic structure calculations, the self-consistent electrostatic potential is handled by Fourier transform. Since the supercell is periodically repeated throughout the whole space, the constant term corresponding to the vacuum energy level of the Fourier transform is not defined. While the vacuum level is irrelevant for neutral systems as it is cancelled out in the total energy expression [22], the total energy does depend on its value for a

* Corresponding author at: Center for Computational Materials, Institute for Computational Engineering and Sciences, University of Texas, Austin, TX 78712, USA. Tel.: +1 512 232 9083; fax: +1 512 471 8694.

E-mail addresses: tlachan@hkbu.edu.hk (T.-L. Chan), ajemyunglee@gmail.com (A.J. Lee), jrc@ices.utexas.edu, jrc.ices@gmail.com (J.R. Chelikowsky).

http://dx.doi.org/10.1016/j.cpc.2014.02.020
0010-4655/

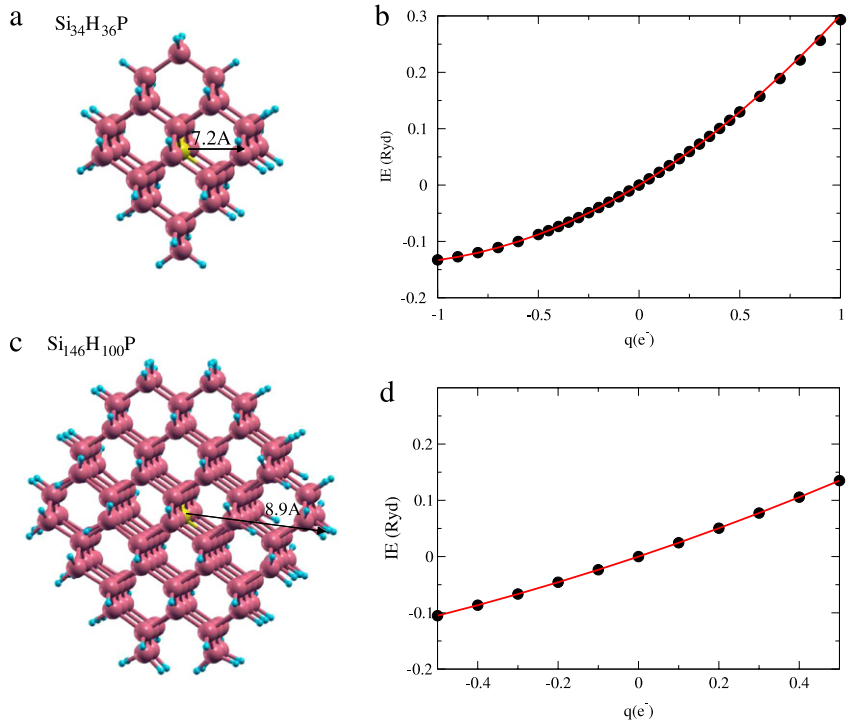

Fig. 1. Ionization of P-doped Si nanocrystals with the confined boundary condition. (a) The geometry of a $Si_{34}H_{36}P$ nanocrystal. The lightly shaded atom at the center is the P dopant, and the dangling bonds of the Si nanocrystal are passivated by small H atoms. The arrow indicates an approximate radius of the nanocrystal. (b) The data points are the ionization energies *IE* as a function of charge state *q* calculated using the confined boundary condition. The curve is a least-square fit using Eq. (1). The same plots are depicted for a $Si_{146}H_{100}P$ nanocrystal in (c) and (d).

charged system. The vacuum level can be specified by aligning the electrostatic potential of a small region of the supercell to a physically meaningful value. A case study on ZnO and GaAs suggests that the MP correction together with potential alignment can lead to well-converged formation energies of charged defects after the finite-size effects unrelated to electrostatic interactions are eliminated [23]. Based on an analysis of the electrostatics in dielectric media, Freysoldt et al. derived a more rigorous correction scheme for the electrostatic interaction between supercells and the correction due to the potential alignment [24].

Here we present an alternative perspective of this charged defect problem. A defect in a crystalline material introduces defect levels within the energy gap of a crystalline semiconducting material. For small variations of its charge state, we regard the defect level as an effective electron reservoir. The addition or extraction of an electron from the defect level can thus be characterized by a work function *W* and a capacitance *C*. Upon charging, a potential difference builds up within the material and contributes to the ionization energy of the defect. Due to the long-ranged Coulomb interaction between periodic ionized defects, both *W* and *C* depend on the supercell size *L*, and lead to the size dependence of the ionization energy *IE* of a defect. By examining the trends of *W* and *C* with respect to *L*, a correction to *W* and *C* can be inferred and results in a correction for *IE*. We shall show that the correction due to *W* is equivalent to the potential alignment, and the correction formula for *C* can be related to the MP correction. Our scheme not only provides an alternative description of the popular MP scheme, but also suggests that a charged defect has a finite size, which should not be treated as a point charge in a dielectric medium as in the MP correction formula. The capacitances suggested in our scheme can be utilized to align the electronic band structure of the ionized defect against the neutral system. Our scheme is first validated by comparing the ionization energy of a P-doped Si nanocrystal calculated using a confined boundary condition (*i.e.* no periodicity imposed) with that calculated by the three dimensional (3D) periodic boundary condition. The scheme is then applied to crystalline Si, where the ionizations of a shallow P substitutional dopant and a deep isolated vacancy are examined.

Our calculations are based on PARSEC [25,26], which is a real-space electronic structure code for density functional calculations (DFT) [27,28]. The local density approximation (LDA) using the Ceperley and Alder exchange–correlation functional [29] parameterized by Perdew and Zunger [30] is employed. Since the ionization energy of P in Si is insensitive to spin polarization (the error is less than 0.02 eV), the calculations are not spin polarized. The ion-core potentials are based on the Troullier–Martins pseudopotentials [31] in the Kleinman–Bylander form [32]. The real space grid is set to be 0.7 a.u., which is sufficient to model the ionization of P and Si. Since the goal is to simulate isolated defects, sufficiently large supercells are employed such that only the Γ point is used for the *k*-point sampling. Atomic structures are relaxed such that the force on each atom is less than 0.001 Ryd/Bohr.

2. Ionization energy of a P-doped Si nanocrystal

To demonstrate the idea, we evaluate the ionization energies *IE* of a small hydrogen-passivated P-doped $Si_{34}H_{36}P$ nanocrystal as illustrated in Fig. 1(a). For the confined boundary condition, the system is enclosed by a spherical domain where the wave function is set to be zero at the boundary. $IE(q) = E(q) - E(0)$ is found by the difference in the total energies of the nanocrystal between charge state *q* and the neutral state. The equation

$$IE(q) = Wq + \frac{q^2}{2C} + \Delta E_{relax} \tag{1}$$

describes the trend as depicted in Fig. 1(b). If a small amount of charges ($|q| < 1$) are added or extracted, then the defect level within the Si energy gap can be regarded as an electron reservoir, and the system is effectively metallic in this small *q* regime. The energetics of charging a piece of metal can be described by

its work function and a geometry-dependent capacitance. Eq. (1) can be interpreted analogously. The linear term in q is an effective work function W, and the quadratic term is an effective capacitance C of the system. The solid line in Fig. 1(b) is a best fit curve using only the q and q^2 terms. W is fitted to be 0.215 Ryd, which is nearly the same as the eigenvalue of the defect level. C is found to be 5.94 e^2/Ryd. From electrostatics, the capacitance of an isolated metallic sphere of radius R is $R/2$ (in atomic units), which implies that $R = 6.3$ Å. Since the electron is drawn from the defect state, the value of C should reflect the effective radius of the defect wave function, which corresponds to the geometrical radius of the $Si_{34}H_{36}P$ nanocrystal. An approximate radius of the nanocrystal (∼7.2 Å) is indicated in Fig. 1(a) as a comparison. The deviation of the calculated data points from the fitted line is small in Fig. 1(b), and can be accounted by ΔE_{relax} originating from the electronic and atomic relaxation due to the ionization. As another illustration, we calculate the capacitance of a larger P-doped $Si_{146}H_{100}P$ nanocrystal. C is found to be 8.35 e^2/Ryd, and implies $R = 8.8$ Å, which corresponds to the geometrical size of the larger nanocrystal very well (see Fig. 1(c) and (d)).

Although fractional electron charges are not physically permissible, they can be interpreted in a statistical sense. For example, half an electron can correspond to a linear combination of two systems, and a full electron has a probability of 50% of residing on one of the systems, see Refs. [33–36] for a review of the subject. The convexity of the total energy versus q curve depends on the DFT functional. If the DFT functional is exact, the curve should exhibit a piecewise-linear behavior with linear segments connecting the integral q. A convex curve is typically obtained for commonly used approximate density functionals such as LDA, GGA or hybrid functionals. Here, we demonstrated that C (the convexity) can be related to the size of the defect wave function and the nanocrystal when LDA is adopted; however, C should not be understood as a physical capacitor, and it may not even have a physical interpretation for other functionals. Nevertheless, C is a measure of the response of the system to charging. As we shall see, since our purpose is to examine the trend of C as a function of the system size with periodic boundary conditions, the exact value and physical meaning of C are in fact not crucial.

How will W and C change if a 3D periodic boundary condition is imposed on the system instead? The $Si_{34}H_{36}P$ nanocrystal is now encased by a cubic box of length L which is periodically repeating in all 3 directions. The IE analysis is performed for different L with a varying amount of vacuum space between the periodic images. Fig. 2(a) reveals that both the slope (W) and the curvature (C) of the IE curves change with L. For a 3D periodic system, it is conventional to remove the divergence in the total energy by setting the average electrostatic potential of the system to be the reference zero V_0 [22]. This is often interpreted as the addition of a neutralizing homogeneous charge background (jellium background) and is equivalent to it. As the system is ionized, the average shifts and V_0 shifts correspondingly. Moreover, the average potential changes with the amount of vacuum space included, hence the shift is L dependent. Since $E(0)$ and $E(q)$ are calculated with respect to different V_0, $IE(q)$, W, and C become erroneous. Although the error diminishes as L increases, the convergence with L is slow. W and C can be corrected leading to a correction of $IE(q)$. Fig. 2(b) illustrates the radial dependence of the self-consistent potential $V(r)$ of the neutral nanocrystal for $L = 48$ a.u. Due to the choice of V_0, the vacuum level is not zero. To infer the true work function W_0, the vacuum level is subtracted by the Fermi level E_F of the system as in Ref. [37]. For L sufficiently large, W_0 converges to the work function extracted from the calculation using the confined boundary condition. Fig. 2(c) presents the trend of W and W_0 with L. The difference between the two curves $\Delta W = W_0 - W$ is the correction to the work function W. Note that, this correction is equivalent to the potential alignment method which aligns $V(r)$ far away from the defect to a desired energy level [38–40].

In Fig. 2(d), C calculated using the 3D periodic boundary condition slowly converges from above to the capacitance of the system inferred using the confined boundary condition, denoted as C_∞. For 3D periodic systems, V_0 of the electrostatic potential shifts with charging; the effect is therefore reflected in C. Consider the shift as an effective capacitance C_{eff} connected in series to C such that

$$\frac{1}{C} + \frac{1}{C_{eff}} = \frac{1}{C_\infty}. \tag{2}$$

Using the calculated C and C_∞, C_{eff} is plotted as a function of L in the inset of Fig. 2(d). The L dependence is found to be linear. This implies that C has an L dependence of the form $1/C = 1/C_\infty - 1/A\,(L + L_0)$. A priori knowledge of C_∞ is usually unavailable. Thus, the black solid curve in Fig. 2(d) corresponds to a fitting of Eq. (2) treating all A, L_0, and C_∞ as parameters. The best fit curve matches the data points very well. C_∞ is fitted to be 5.76 e^2/Ryd, which is close to 5.94 e^2/Ryd obtained via the confined boundary condition. Therefore, a varying V_0 in 3D periodic calculations effectively enhances the capacitance of a system leading to an underestimation of IE. A correction of IE due to the effective capacitance is $\Delta E_{cap} = q^2/2C_{eff}$.

The total correction of IE for 3D periodic systems is:

$$IE_c(q) = E(q) - E(0) + q\Delta W + \frac{q^2}{2C_{eff}}. \tag{3}$$

The resultant $IE_c(+1)$ as a function of L is plotted in Fig. 2(e). $IE_c(+1)$ converges to 4.06 eV instead of the true value 3.99 eV. This is because $IE_c(+1)$ trends to a value that is consistent with the inferred values of W_0 and C_∞ using information extracted from the calculations with different L. However, the error is only ∼2%. IE_c already includes the effect of atomic relaxation because both $E(q)$ and $E(0)$ correspond to total energies after the system is relaxed. MP suggested a correction of the form $\alpha q^2/\epsilon L$, where α is the Madelung constant and ϵ is the static dielectric constant of the material [3]. Eq. (3) implies that $C_{eff} = \epsilon L/2\alpha$, where C_{eff} is directly proportional to L. However, our analysis indicates that the dependence on L can be more accurately described by the form $A\,(L + L_0)$. As L trends to 0, the MP correction diverges. This is because the correction corresponds to the Madelung energy of a lattice of point charges immersed in a jellium background. If an ionized defect does not correspond to a point charge, then C_{eff} should not diminish as L approaches 0. By replacing the quadratic term in Eq. (3) with $\alpha q^2/\epsilon L$ ($\alpha = 2.8373$ for simple cubic lattice, $\epsilon = 1$ for vacuum) while keeping the linear term (or the potential alignment) the same, the resultant ionization energies $IE_{MP}(+1)$ versus L is plotted in Fig. 2(e) as a comparison. The difference between $IE_c(+1)$ and $IE_{MP}(+1)$ is small and within 0.03 eV. However, $IE_{MP}(+1)$ has a very soft L dependence that is absent in $IE_c(+1)$, which can be attributed to the lack of L_0 in the MP scheme.

The shift of V_0 in a 3D periodic calculation not only affects IE, but also the alignment of the electronic band structure. Fig. 2(f) presents the eigenvalue spectrum of the nanocrystal calculated using the 3D periodic boundary condition. The spectrum with $q = +1$ is shifted downwards roughly by q/C compared to the neutral case. A correct alignment is to adjust the spectrum further downwards for q/C_{eff} as indicated in Fig. 2(f). If both the neutral and $q = +1$ spectrums are also shifted uniformly downwards by an amount ΔW, then the resulting spectrums will be nearly exactly the same as those calculated using the confined boundary condition. The shift by q/C_{eff} is to align the eigenvalue spectrum of a charged system with respect to that of the neutral system, while the shift by ΔW is to align both spectrums such that V_0 is located in the vacuum infinitely far away. Therefore, an advantage of utilizing C is that it can both correct the total energy and the eigenvalue spectrum of a charged periodic system.

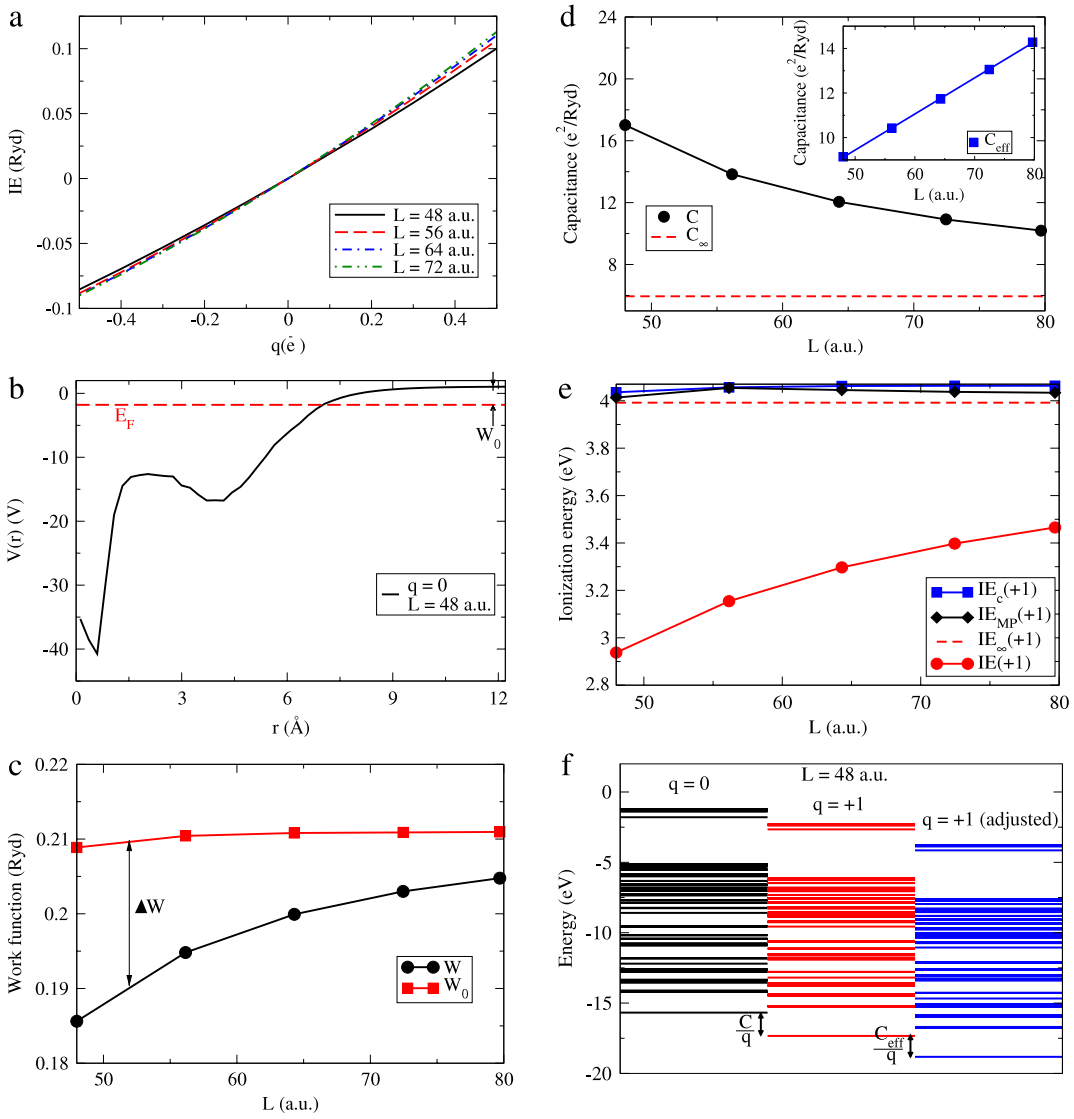

Fig. 2. Ionization of a P-doped Si nanocrystal with periodic boundary conditions. (a) Same as Fig. 1(b) but with the 3D periodic boundary condition. (b) The self-consistent potential $V(r)$ of the neutral nanocrystal as a function of the radial distance r. The difference between $V(r)$ inside the vacuum and the Fermi level of the system E_F gives the true work function W_0. (c) The difference between the effective work function W inferred from (a) and W_0 is ΔW. (d) The data points depict C as a function of L with the connecting curve fitted using Eq. (2). C_{eff} and C_∞ are obtained from the fitting. The inset illustrates the L dependence of C_{eff}. (e) The ionization energy for the extraction of 1 electron from the nanocrystal $IE(+1)$ can be corrected by Eq. (3) to give $IE_c(+1)$. $IE_{MP}(+1)$ is obtained using the Makov–Payne correction. $IE_\infty(+1)$ is the true value of the ionization energy calculated using the confined boundary condition. (f) A comparison of the eigenvalue spectrums between a neutral ($q = 0$) and a charged ($q = 1$) nanocrystal. The eigenvalue spectrum of the charged nanocrystal should be adjusted by C_{eff}/q such that it is correctly aligned to the neutral case.

3. Application to crystalline materials

Eq. (3) can be applied to crystalline materials as well. Consider the ionization of a P donor in crystalline Si as illustrated in Fig. 3(a). As P is a shallow donor, its defect wave function is very extended. This is problematic for our method if the wave function cannot be contained within the supercell. On the other hand, since the magnitude of C correlates with the extent of the wave function, a delocalized wave function implies a large C and a correspondingly small energy correction. When IE is plotted against q in Fig. 3(a) for $L = 51.6$ a.u., the curve is nearly a straight line, and confirms that C is indeed very large. Although the value of C cannot be reliably extracted, ΔE_{cap} is practically 0. Another notable feature is that the trend has a negative slope in contrast to Fig. 2(a), hence implying a negative W. This stems from the fact that modeling a crystalline material with the 3D periodic boundary condition does not include the surface/vacuum interface and lacks an explicit vacuum level. When E_F is higher than the average of the electrostatic potential, which is taken to be the reference zero V_0, W becomes negative.

For the work function correction, what should be W_0? As in the case of nanocrystals, the defect electron can be extracted from the bulk to the vacuum infinitely far away; however, the corresponding W_0 has to be acquired from the experimental data since a 3D periodic simulation of a crystalline material does not contain information regarding the vacuum level as explained above. For electronics applications, the ionization of an n-type dopant does not usually involve extracting an electron to the vacuum, but to the conduction band minimum (CBM) of the embedding semiconductor. As such, rather than choosing the vacuum level to be the reference of the work function, the eigenvalue of CBM in pure crystalline Si E_{CBM} is selected instead. E_{CBM} is obtained by a separate calculation of pure crystalline Si. Therefore, $W_0 = E_{CBM} - E_F$, where E_F is the Fermi level of the neutral P-doped crystalline Si. Note that the assignment of the reference E_{CBM} for W_0 is not unique. In general, the reference corresponds to the energy level of an electron reservoir where the defect electron can go after the dopant is ionized. It should be chosen such that it is relevant to the system of interest.

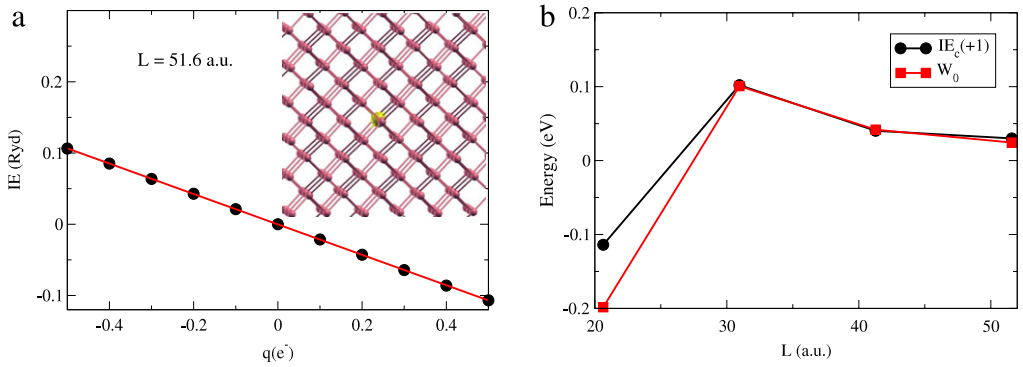

Fig. 3. Ionization of P in crystalline Si. (a) *IE* of P-doped crystalline Si as a function of q for $L = 51.6$ a.u. The plots for other values of L are similar (not shown for clarity) except the slopes are slightly different. The inset illustrates the geometry of a P-doped Si bulk crystal. (b) The corrected ionization energies $IE_c(+1)$ as a function of L. The corresponding trend of W_0 is also depicted for comparison.

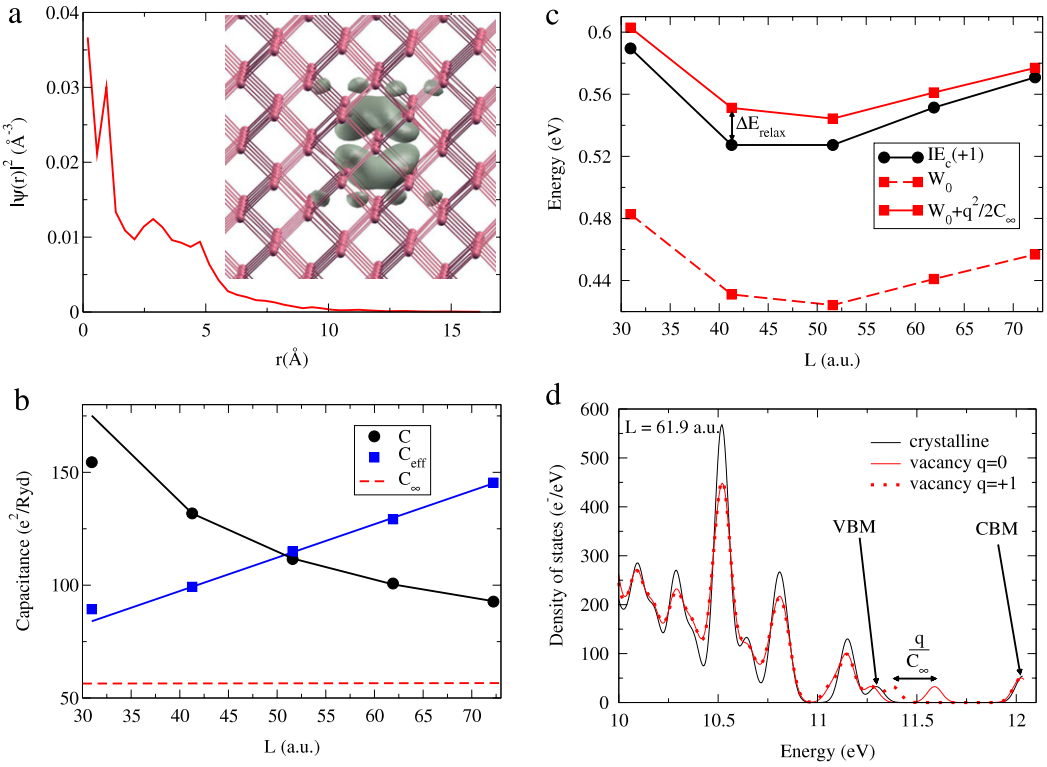

Fig. 4. Ionization of a Si vacancy. (a) The geometry of crystalline Si with an isolated vacancy at the center. Overlapped on the geometry is a surface contour of the vacancy defect wave function inside the Si energy gap. The radial dependence of the defect wave function is also illustrated. (b) L dependence of the capacitance C and C_{eff}. The asymptotic value of C is C_∞. (c) The corrected ionization energy $IE_c(+1)$ is plotted as a function of L. The work function W_0 with and without the contribution from the capacitance ($q^2/2C_\infty$) are also illustrated. (d) An alignment of the electronic band structure of a charged vacancy to the neutral one.

While the correction by $\Delta W = W_0 - W$ is equivalent to a potential alignment, the alignment process is not unique. Typically, one can average the self-consistent potential (or just its electrostatic part) over a region far away from the defect and align it to a similar region from another calculation. An advantage of the ΔW correction instead of the potential alignment is that the work function W is calculated from the total energies, there is relatively little arbitrariness on how it is obtained. With $\Delta E_{cap} = 0$, using ΔW as the correction, IE_c is evaluated for 4 different L in Fig. 3(b). If L is not sufficiently large, there is significant interaction between the P defect wave function from periodic images, which affects the resultant IE_c. IE_c is found to be 40 meV and 30 meV for $L = 41.3$ and 51.6 a.u., respectively, and comparable to the experimental value of 45 meV [41]. Fig. 3(b) also shows that IE_c follows W_0 closely. One reason is that the contribution by C_{eff} is negligible for shallow dopants. In addition, $\Delta E_{relax} \sim 0$ for this particular system.

The simplification of $IE_c \sim W_0$ is not applicable if the defect level is deep within the energy gap. As an example, consider an isolated vacancy in crystalline Si. To demonstrate our scheme, a D_2 symmetry is imposed on the atomic configuration of the vacancy to avoid the formation of a dipole moment within the unit cell. Non-spin-polarized calculations are still adopted in this case because the focus here is just to demonstrate how IE_c varies with L. Moreover, our results should not be compared with experimental measurements without corrections of the LDA gap error. As shown in Fig. 4(a), the defect wave function is localized within 1 nm around the vacancy. By examining the linear part of the *IE* versus q curve, W can be extracted. If we consider the vacancy as a donor, $W_0 = E_{CBM} - E_F$ as for the case of P-doped Si. The capacitance associated with ionizing the vacancy is related to the size of the defect wave function multiplied by the dielectric constant of Si. Thus, the resultant capacitance is large compared to the P-doped Si nanocrystal, which is embedded in vacuum. Instead of

extracting C from the curvature of the IE curve, it is more reliable to plot the variation of the Fermi level of a charged vacancy $E_F(q)$ with q and use its linear slope as an estimate of $1/C$. This is because $E_F \approx \Delta IE/\Delta q$ by Janak's theorem [42,43], hence $E_F(q) \approx W + q/C$ from Eq. (1). The resultant C is plotted in Fig. 4(b), and the solid black curve is fitted using Eq. (2). The linearity of C_{eff} versus L originates from the shift of the vacuum level V_0. For small L, C can also be modified by the significant interactions among the vacancies as the defect wave function overlaps. The resultant C_{eff} curve becomes non-linear as seen in Fig. 4(b). Nevertheless, the linearity quickly recovers for sufficiently large L. The inferred value of C_∞ is 56.6 e^2/Ryd. If we envision the ionization of a vacancy as charging up a sphere with capacitance $\epsilon R/2$, then the vacancy has an effective radius $R \sim 5.1$ Å using the experimental value of the Si dielectric constant $\epsilon = 11.7$. R corresponds quite well to the extent of the defect wave function in Fig. 4(a), which spreads over a couple Si bond lengths. Finally, IE_c is evaluated using Eq. (3) and plotted in Fig. 4(c). For $L = 61.9$ and 72.2 a.u., $IE_c = 0.55$ and 0.57 eV, respectively. Unlike a shallow donor, IE_c is not well approximated by W_0 as $q^2/2C_\infty$ is not negligible, and ΔE_{relax} contributes to the ionization energy for vacancies. The ionization energies of deep donors cannot be inferred from the eigenvalues, or the error can be as large as 20% from Fig. 4(c).

Compared to the MP correction, our scheme does not require a separate evaluation of the static dielectric constant ϵ of the crystalline material. C_{eff} and C_∞ already include the contribution by ϵ. In addition, the knowledge of C_{eff} suggests how the electronic band structure of a charged system should be aligned to the neutral one as for the case of the P-doped Si nanocrystal. For nanocrystals, C_∞ determines the voltage of the nanocrystal with respect to the underlying vacuum upon charging. Analogously, for crystalline materials that contain bulk states infinite in extent, C_∞ corresponds to an effective voltage between the spatially localized electronic levels and the extended bulk states. Since $C \neq C_\infty$ for finite L, the localized levels are not properly aligned with respect to the bulk. Bulk extended states can be aligned with respect to the vacuum by making use of the work function of the bulk material. However, the purpose here is just to align the ionized defect level with respect to the bulk. As such, we keep the bulk electronic levels intact but shift the defect levels down in energy by q/C_{eff}. The resultant electronic structure of a charged vacancy is compared to that of a neutral vacancy in Fig. 4(d).

4. Conclusions

We proposed to examine an effective work function and capacitance for a charged 3D periodic system. The effective work function is equivalent to the potential alignment method, while the effective capacitance gives rise to an expression similar to the Makov–Payne correction. The validity of our scheme is first demonstrated for the ionization of a P-doped Si nanocrystal. The charged nanocrystal can be calculated using either a confined boundary condition or a 3D periodic boundary condition. An analysis based on the effective capacitance approach indicates that an ionized defect can be better described by a charged particle of finite size rather than a point charge. The voltage implied by the capacitance provides a convenient alignment of electronic band structures between charged and neutral systems. We then apply our scheme to P-doped crystalline Si, where P is a shallow donor. For the ionization of a shallow dopant, a correction to the total energy due to the effective work function is already sufficient as the effective capacitance is large for an extended defect wave function. For deep defects in a crystalline material, we examine the ionization of an isolated vacancy in crystalline Si as a case study. As the defect wave function is localized in space, a voltage builds up between the ionized defect and the embedding host material. Thus, both corrections due to the effective work function and capacitance contribute to the ionization energy. For crystalline materials, the screening by the host material through the dielectric constant is already included in the capacitance, and does not need to be evaluated separately as in the Makov–Payne scheme.

Acknowledgments

We would like to acknowledge the partial support from the U.S. Department of Energy (DoE) for the work on nanostructures from grant DE-FG02-06ER46286, and the support provided by the Scientific Discovery through Advanced Computing (SciDAC) program funded by U.S. DoE, Office of Science, Advanced Scientific Computing Research and Basic Energy Sciences under award number DESC0008877 on algorithms. Computational resources are provided in part by the National Energy Research Scientific Computing Center (NERSC) and the Texas Advanced Computing Center (TACC). T.L. Chan acknowledges computational resources provided by the High Performance Cluster Computing Center (HPCCC) at Hong Kong Baptist University, which receives funding from the Research Grant Council, University Grant Committee of the HKSAR and the Hong Kong Baptist University.

References

[1] W.R.L. Lambrecht, Phys. Status Solidi (b) 248 (2011) 1547–1558.
[2] M. Leslie, M.J. Gillan, J. Phys. C 18 (1985) 973.
[3] G. Makov, M.C. Payne, Phys. Rev. B 51 (1995) 4014.
[4] A.F. Wright, N.A. Modine, Phys. Rev. B 74 (2006) 235209.
[5] C.W.M. Castleton, A. Höglund, S. Mirbt, Phys. Rev. B 73 (2006) 035215.
[6] P.E. Blöchl, J. Chem. Phys. 103 (1995) 7422.
[7] P.A. Schultz, Phys. Rev. B 60 (1999) 1551.
[8] P.A. Schultz, Phys. Rev. Lett. 84 (2000) 1942.
[9] R.N. Barnett, U. Landman, Phys. Rev B 48 (1993) 2081.
[10] D. Marx, J. Hutter, M. Parrinello, Chem. Phys. Lett. 241 (1995) 457.
[11] G.J. Martyna, M.E. Tuckerman, J. Chem. Phys. 110 (1999) 2810.
[12] M.R. Jarvis, I.D. White, R.W. Godby, M.C. Payne, Phys. Rev. B 56 (1997) 14972.
[13] C.A. Rozzi, D. Varsano, A. Marini, E.K.U. Gross, A. Rubio, Phys. Rev. B 73 (2006) 205119.
[14] S. Ismail-Beigi, Phys. Rev. B 73 (2006) 233103.
[15] I. Dabo, B. Kozinsky, N.E. Singh-Miller, N. Marzari, Phys. Rev. B 77 (2008) 115139.
[16] R. Rurali, X. Cartoixà, Nano Lett. 9 (2009) 975.
[17] R. Rurali, M. Palummo, X. Cartoixà, Phys. Rev. B. 81 (2010) 235304.
[18] J. Neugebauer, M. Scheffler, Phys. Rev. B 46 (1992) 16067.
[19] L. Bengtsson, Phys. Rev. B 59 (1999) 12301.
[20] A. Natan, L. Kronik, Y. Shapira, Appl. Surf. Sci. 252 (2006) 7608.
[21] A.Y. Lozovoi, A. Alavi, Phys. Rev. B 68 (2003) 245416.
[22] J. Ihm, A. Zunger, M.L. Cohen, J. Phys. C: Solid State Phys. 12 (1979) 4409.
[23] S. Lany, Alex Zunger, Phys. Rev. B 78 (2008) 235104.
[24] C. Freysoldt, J. Neugebauer, C.G. Van de Walle, Phys. Rev. Lett. 102 (2009) 016402.
[25] J.R. Chelikowsky, J. Phys. D 33 (2000) R33.
[26] PARSEC has a website at http://parsec.ices.utexas.edu.
[27] P. Hohenberg, W. Kohn, Phys. Rev. 136 (1964) B864.
[28] W. Kohn, L.J. Sham, Phys. Rev. 140 (1965) A1133.
[29] D.M. Ceperley, B.J. Alder, Phys. Rev. Lett. 45 (1980) 566.
[30] J.P. Perdew, Y. Wang, Phys. Rev. B 45 (1992) 13244.
[31] N. Troullier, J.L. Martins, Phys. Rev. B 43 (1991) 1993.
[32] L. Kleinman, D.M. Bylander, Phys. Rev. Lett. 48 (1982) 1425.
[33] J.P. Perdew, R.G. Parr, M. Levy, J.L. Balduz Jr., Phys. Rev. Lett. 49 (1982) 1691.
[34] A.J. Cohen, P. Mori-Sánchez, W. Yang, Chem. Rev. 112 (2012) 289–320.
[35] J.C. Slater, The self-consistent field for molecules and solids, in: Quantum Theory of Molecules and Solids, vol. 4, McGraw-Hill, 1974.
[36] E. Kraisler, L. Kronik, Phys. Rev. Lett. 110 (2013) 126403.
[37] C.J. Fall, N. Binggeli, A. Baldereschi, J. Phys.: Condens. Matter 11 (1999) 2689–2696.
[38] C. Persoon, Y.J. Zhao, S. Lany, A. Zunger, Phys. Rev. B 72 (2005) 035211.
[39] D.B. Laks, C.G. Van de Walle, G.F. Neumark, P.E. Blöchl, S.T. Pantelides, Phys. Rev. B 45 (1992) 10965.
[40] T. Mattila, A. Zunger, Phys. Rev. B 58 (1998) 1367.
[41] S.M. Sze, Semiconductor Devices: Physics and Technology, third ed., Wiley, 2012.
[42] J.F. Janak, Phys. Rev. B 18 (1978) 7165.
[43] T. Koopmans, Physica 1 (1934) 104–113.